

1        **Development Processes of Oceanic Convective Systems**  
2        **Inducing the Heavy Rainfall over the Western Coast of**  
3        **Sumatra on 28 October 2007**

4

5        Trismidianto<sup>1,2</sup>, Tri Wahyu Hadi<sup>3</sup>, Sachinobu Ishida<sup>1</sup>, Atsuyoshi Manda<sup>4</sup>, Satoshi  
6        Iizuka<sup>5</sup>, and Qoosaku Moteki<sup>6</sup>

7        <sup>1</sup>*Meteorological Laboratory, Graduate School of Science and Technology, Hirosaki*  
8        *University, Hirosaki, Japan*

9        <sup>2</sup>*Center of Atmospheric Science and Technology, National of Aeronautics and Space*  
10        *(LAPAN), Jakarta, Indonesia*

11        <sup>3</sup>*Departement of Earth Sciences, Faculty of Earth Sciences and Technology, Institut*  
12        *Teknologi Bandung, Bandung, Indonesia*

13        <sup>4</sup>*Graduate School of Fisheries Science and Environmental Studies, Nagasaki University,*  
14        *Nagasaki, Japan*

15        <sup>5</sup>*Monitoring and Forecast Research Department, National Research Institute for Earth*  
16        *Science and Disaster Prevention, Tsukuba, Japan*

17        <sup>6</sup>*Japan Agency for Marine-Earth Science and Technology, Yokosuka, Japan*

18

19        Corresponding author: Trismidianto, Graduate School of Science and Technology,  
20        Hirosaki University, 3 Bunkyo-cho, Hirosaki-shi, Aomori 036-8561, Japan. E-mail:  
21        h132ds252@hirosaki-u.ac.jp.

22

23

24

25

## Abstract

26 This study analyzed the oceanic convective systems that induced heavy rainfall over the  
27 western coast of Sumatra on 28 October 2007. The convective systems that satisfied the  
28 definition of a mesoscale convective complex (MCC), as identified by infrared satellite  
29 imagery, developed repeatedly for 16 hours over the Indian Ocean near Sumatra. The  
30 MCC developed from midnight on 27 October until the early morning of 28 October,  
31 and it was intensified by the land breeze from Sumatra. New convective systems around  
32 the decaying MCC were generated during the daytime of 28 October, and they  
33 propagated to the western coast of Sumatra in the evening because of a divergent  
34 outflow from a cold pool. The combination of the land breeze from Sumatra and cold  
35 pool outflows from the decaying MCC was a significant factor in the formation of the  
36 convective system that induced strong rainfall up to  $46 \text{ mm h}^{-1}$  over the western coast  
37 of Sumatra.

38

## 39 1. Introduction

40 The Indonesian Maritime Continent (IMC) is the area of greatest convective  
41 activity within the tropics, and it receives the largest amount of rainfall of anywhere in  
42 the world (Ramage 1968). Sumatra is one region within the IMC where deep convection  
43 occurs frequently (Yamanaka et al. 2008), generating the largest volumetric rainfall  
44 especially on the western coast of Sumatra (Hirose et al. 2009; Love et al. 2011). Mori  
45 et al. (2011) showed that average annual rainfall greater than  $3,000 \text{ mm y}^{-1}$  on 10-year  
46 period (1998-2007) was observed along the southwestern coast of Sumatra. Sumatra is  
47 the second region most frequently floods within Indonesia which approximately 1401

48 flood events recorded during the 13-year period from 2002 to 2014, and about 38.62%  
49 of those occurred on the western coast of Sumatra based on data from the National  
50 Board for Disaster Management (*source data: <http://dibi.bnpb.go.id/>*).

51 Many previous studies have described the characteristics and propagation of the  
52 diurnal convection near Sumatra (e.g., Mori et al. 2004; Sakurai et al. 2005). Mori et al.  
53 (2004) showed that diurnal convection, which develops over the western coast of  
54 Sumatra in the late evening, could migrate up to 400 km from the coastline under the  
55 influence of low-level westerly winds. Generally, diurnal convection develops over the  
56 mountainous region of Sumatra because of strong daytime surface heating, although  
57 larger-scale convective systems are sometimes organized by interactions between land  
58 and sea breeze circulations and large-scale environment flows (Nitta and Sekine 1994;  
59 Mori et al. 2004). Shibagaki et al. (2006) showed that westward-propagating meso- $\beta$ -  
60 scale cloud clusters (horizontal scale of  $\sim 100$  km) that develop in the eastern  
61 mountainous region of Sumatra, can act as triggers for the development of larger-scale  
62 systems, the so-called super cloud clusters (Nakazawa 1988). Houze et al. (1981) have  
63 documented that convection over the island of Borneo, related to sea breeze  
64 convergence, is able to aggregate and move off the coast to produce the greatest amount  
65 of precipitation during the morning over the oceans (Williams and Houze 1987).

66 There are several definitions of convective systems depending on the parameters  
67 used and several phrases used to describe them, e.g., mesoscale convective systems  
68 (MCSs), mesoscale convective complexes (MCCs), as the largest subclass of MCSs  
69 (Maddox 1980), and super cloud clusters (Nakazawa 1988). Here, for ease of  
70 comparison with previous studies, the definition of the MCC based on a universal rule  
71 using only satellite data. Several previous studies (e.g., Yuan and Houze 2010; Virts and

72 Houze 2015) have documented the climatology of the largest MCSs over the entire area  
73 of the tropics, including the IMC, and they have identified the existence of MCCs over  
74 the Indian Ocean. However, there have been few studies analyzing the surface winds  
75 around MCCs in the tropics because observations over the ocean are too sparse to detect  
76 the detailed surface wind distribution.

77 This study focused on the elucidation of the role of the MCC that occurred over  
78 the Indian Ocean near Sumatra on 27–28 October 2007 in inducing the generation of  
79 new convective systems that produce heavy rainfall on the western coast of Sumatra.  
80 Analysis of Cross Calibrated Multi Platform (CCMP) data was attempted to give a  
81 deeper insight into the mechanism of eastward-propagating convective systems, which  
82 previously have been reported to occur in the region (e.g., Mori et al. 2004). The effect  
83 of the cold pool from the decaying MCC and its interaction with the land and sea breeze  
84 circulations are the subjects of discussions in this article.

85

## 86 **2. Data and study method**

87 The equivalent black body temperature ( $T_{BB}$ ), derived from the hourly infrared  
88 data of MTSAT-1R (Multi-functional Transport Satellite) with spatial resolution of  
89  $0.05^\circ \times 0.05^\circ$ , was used to identify the MCCs and their physical characteristics based on  
90 the parameters given by Maddox (1980) as shown in Table 1. In addition, the  
91 convective index ( $C_1$ ) was determined by taking the temperature below a threshold value  
92 if  $T_{BB}$  was smaller than the threshold value ( $C_1 = \text{threshold} - T_{BB}$ , for  $T_{BB} < \text{threshold}$ )  
93 and making  $C_1$  equal to zero for  $T_{BB}$  values that were greater than or equal to the  
94 threshold value ( $C_1 = 0$ , for  $T_{BB} \geq \text{threshold}$ ). In this study, the threshold value was set at  
95 253 K as suggested by Adler and Negri (1988). The estimated rainfall data,

96 corresponding to the MCCs, were obtained from the Tropical Rainfall Measuring  
97 Mission's (TRMM) 3B42 v6 data set, which has 3-hourly temporal resolution and  $0.25^\circ$   
98  $\times 0.25^\circ$  spatial resolution.

99 The surface wind data were obtained from the CCMP, which covers the global  
100 ocean for the period of 20-years with 6-hourly temporal resolution and 25-km spatial  
101 resolution. The dataset is produced using a variational analysis method to combine  
102 extensive cross-calibrated multiple satellite datasets with in situ data and ECMWF  
103 (European Centre for Medium-Range Weather Forecasts) analyses (Atlas et al. 2011).  
104 In order to identify the cloud-induced surface flows, wind vector anomalies were  
105 calculated by subtracting the resultant daily wind speed from the 6-hourly wind speed.  
106 The existence of cold pool was examined using the **surface** potential temperature from  
107 the ECMWF ERA-Interim analysis fields, which are available at 6-hourly intervals with  
108  $0.25^\circ$  horizontal resolution (Dee et al. 2011).

109 The representativeness of the TRMM and ERA-Interim data over land were  
110 assessed by comparing with observational data obtained at Pulau Baai weather station in  
111 Bengkulu ( $3.47^\circ\text{S}$ ,  $101.80^\circ\text{E}$ ) and synoptic data over Sumatra from several weather  
112 stations, i.e., at Tabing in Padang ( $0.53^\circ\text{S}$ ,  $100.21^\circ\text{E}$ ), Simpang-tiga in Pekanbaru  
113 ( $0.28^\circ\text{N}$ ,  $101.27^\circ\text{E}$ ), and Padang Kemiling in Bengkulu ( $3.53^\circ\text{S}$ ,  $102.20^\circ\text{E}$ ) obtained  
114 from the OGIMET meteorological database (Valor and López 2014). The temporal  
115 trend of the global data was confirmed to be consistent with that of observations from  
116 the several weather stations over Sumatra that shows high correlations of more than 0.7.  
117 Over the ocean, comparison with data obtained **from** TRITON (Triangle Trans-Ocean  
118 buoy Network, Ando et al. 2005) buoy at ( $5^\circ\text{S}$ ,  $95^\circ\text{E}$ ) shows high correlations of more  
119 than 0.7.

120

### 121 3. Results and discussion

#### 122 3.1. Evolution of the development of the MCC

123 Figure 1 shows the evolution of the MCC that occurred near Sumatra on 27–28  
124 October 2007. Cotton et al. (1989) have defined eight stages in the life cycle of an  
125 MCC: MCC-12 h, pre-MCC, initial, growth, mature, decay, dissipation, and post-MCC;  
126 however, the most important period for an MCC is from the initial to the dissipation  
127 stage. The MCC-12 h stage defines the condition of the MCC around 10–15 hours  
128 before the initial stage, as shown in Fig. 1a. In addition, the MCC developed under a  
129 large-scale environmental situation in which the Madden-Julian oscillation index  
130 (Wheeler and Hendon 2004) was positive but its amplitude was very weak.

131 The MCC that is the topic of this study began to develop from the pre-MCC  
132 stage at 2200 local time (LT) on 27 October 2007. At that time, small-scale clouds were  
133 located over the western coast of Sumatra and the nearby Indian Ocean, as shown in Fig.  
134 1b. These groups of clouds grew rapidly until around midnight (0100 LT), which  
135 marked the onset of the initial stage (Fig. 1c). By 0400 LT on 28 October 2007 (Fig. 1d),  
136 during the growth stage of the MCC, the sizes of the clouds had increased further and  
137 they began merging with each other, such that the maximum extent of the MCC was  
138 attained at 0700 LT (Fig. 1e). During the mature stage, the MCC had a cloud shield with  
139 an area of around 319,083 km<sup>2</sup> and the interior cold cloud covered an area of around  
140 211,059 km<sup>2</sup>. The center of the MCC during this stage was around 3.21°S, 97.46°E with  
141 an eccentricity of around 0.76. At 1300 LT, during the decay stage, the MCC began to  
142 split and dissipated (Fig. 1f). During the dissipation stage in the late afternoon (1600  
143 LT) (Fig. 1g) and by the post-MCC stage later that evening (1900 LT) (Fig. 1h), the

144 MCC had split into small-scale clouds that propagated eastward toward the western  
145 coast of Sumatra.

### 146 3.2. *The Development of New Convective Systems*

147 Figure 2a shows that some of the clouds mentioned in subsection 3.1 are  
148 convective clouds indicated by high  $C_I$  values. The convergent surface wind flow  
149 indicates that the land breeze triggered the development of some of the clouds over the  
150 western coast of Sumatra, whereas the westerly wind in the lower atmosphere triggered  
151 the development of some of the clouds over the nearby Indian Ocean. This is consistent  
152 with the findings of Mori et al. (2004) and Sakurai et al. (2005), who concluded that  
153 ocean convection occurs in the morning until noon, owing to the propagation of  
154 convective systems along the western coast of Sumatra, triggered by this strong land  
155 breeze, but in this study, the convective systems discussed are defined as MCC. During  
156 the mature stage of the MCC early in the morning (0700 LT) of 28 October, as shown in  
157 Fig. 2b, some of the clouds over the western coast of Sumatra and the nearby Indian  
158 Ocean merged to create the maximum extent of the MCC. The convergence of the land  
159 breeze and the westerly wind clearly supported the development of the MCC. The  
160 potential temperature at the center of the MCC was relatively low (at around 297.5 K)  
161 compared with the surrounding area (299–300 K). According to Engerer et al. (2008),  
162 this area is the so-called cold pool, which is an area of downdraft air cooled by  
163 evaporation that spreads out horizontally beneath a precipitating cloud. In addition, the  
164 cold pools were associated with potential temperature decreases (Tompkins 2001) and  
165 generated by these individual convective cells in an MCS typically spread out at the  
166 surface and combine to form a large mesoscale cold pool covering a contiguous area on  
167 the scale of the entire MCS (Houze 2004).

168           In this case study, the cold pool began to develop during the mature stage and it  
169 spread increasingly until the decay stage, as shown in Fig. 2c. The difference in  
170 potential temperature could have acted as a trigger for the development of new  
171 convective systems to form along the leading edge of the cold pool, as in frontal theory  
172 (Fig. 2c), which is consistent with the findings of Wilson and Schreber (1986). Such  
173 new convective systems, which are generated over the ocean in the daytime, eastward-  
174 propagating to the western coast of Sumatra due to of the divergent outflow of the cold  
175 pool, in conjunction with the evening sea breeze. Convective activities over Sumatra are  
176 more extensive during the evening (1900 LT) due to the new convective systems induce  
177 the land convection over the western coast of Sumatra (Fig. 2d). Therefore, this study  
178 give a deeper insight into the mechanism of eastward-propagating convective systems,  
179 which previously have been reported to occur in the region (e.g., Mori et al. 2004). The  
180 structure and evolution of MCCs over the Indian Ocean are related to the diurnal  
181 convective activities over Sumatra.

### 182 **3.3. *Diurnal rainfall variation during the MCC event***

183           Figure 3 shows the horizontal distribution of rainfall during the studied MCC  
184 event. During the initial stage at 0100 LT (Fig. 3a), only light rainfall ( $<6 \text{ mm h}^{-1}$ ) was  
185 observed over the Indian Ocean. However, the observed early morning (0700 LT)  
186 maximum occurred because of the increase in the number of convective clouds (Fig. 2a),  
187 rather than because of the increase in extent of the coverage of the MCC during the  
188 mature stage (Fig. 3b). [The rainfall system began to propagate slowly eastward from the](#)  
189 [Indian Ocean toward the western coast of Sumatra \(Fig. 3c\) during the new convective](#)  
190 [systems which generated by MCC propagate eastward to the western coast of Sumatra](#)  
191 [at the decay stages at the daytime \(1300 LT\), and the peak rainfall on the western coast](#)



192 of Sumatra began in the evening at 1600 LT (Fig. 3d) until 1900 LT (Fig. 3e) is caused  
193 by the interaction of new convective systems with land convection which make the  
194 convective activity becomes intense on the western coast of Sumatra during the  
195 dissipation stages until post-MCC stages. Compared with the observational data, the  
196 rainfall intensity increased significantly, especially during the dissipation and the post-  
197 MCC stages over some parts of western Sumatra, as shown in Fig. 4. Heavy rainfall  
198 occurred over southwestern coastal ocean at Pulau Baai (Bengkulu) from 1400–1900  
199 LT, which reached a maximum intensity of around  $35 \text{ mm hr}^{-1}$  at 1600–1700 LT during  
200 the dissipation stage of the MCC. During the post-MCC stage at 1900 LT, a significant  
201 increase in rainfall (up to  $46 \text{ mm h}^{-1}$ ) occurred over southwestern coastal land at Padang  
202 Kemiling (Bengkulu). Rainfall also occurred over northwestern coastal land at Tabing  
203 (Padang) and over inland at Simpang-tiga (Pekanbaru) but it was only light in intensity  
204 because of the weaker effect of the MCC compared with the area around Bengkulu. The  
205 diurnal rainfall associated with the MCC had a similar pattern. The rainfall over the  
206 Indian Ocean occurred when the MCC started developing and it reached a maximum  
207 when the MCC began to decay, at which time, the rain started to move toward the  
208 western coast of Sumatra. This is consistent with previous studies, which have stated  
209 that MCCs possess the potential to exert considerable impact on regional rainfall  
210 patterns, as mentioned in section 1.

211 Schematic representations of the MCCs evolution and migration over the Indian  
212 Ocean, related to the diurnal variation of rainfall over the western coast of Sumatra, are  
213 shown in Fig. 5 based on the results described above. Figure 5a shows the initial stage  
214 of the MCC at around midnight on 28 October 2007. The development of the MCC over  
215 the Indian Ocean began from several convective clouds generated by the land breeze

216 and westerly wind. Figure 5b shows the mature stage of the MCC in the early morning  
217 on 28 October. The MCC reached its maximum extent and the peak rainfall occurred  
218 over the Indian Ocean because of the propagation and merging of several areas of  
219 convective cloud, triggered by the convergence between the land breeze and the  
220 westerly wind. Figure 5c shows the decay and dissipation stages of the MCC, which  
221 occurred during the daytime through to the evening. The MCC began to dissipate and  
222 new convective systems were generated owing to the development of the cold pool. The  
223 new convective system generated over the Indian Ocean during the daytime propagated  
224 to the western coast of Sumatra because of the divergent outflow of the cold pool, in  
225 conjunction with the evening sea breeze.

226         This evolutionary scheme differs from the scenarios outlined previously by Mori  
227 et al. (2004) and Shibagaki et al. (2006), who described the westward propagation of  
228 developing convective systems over Sumatra, as mentioned at the second paragraph in  
229 section 1. However, the convective systems described by Houze et al. (1981) are similar  
230 and they share common features with those of the present study. Houze et al. (1981)  
231 showed that the convective systems over the South China Sea begin to develop around  
232 midnight and mature in the early morning, helped by the land breeze from the island of  
233 Borneo to the east. This study presented a more detailed evolution of the MCCs in the  
234 IMC region and a description of the convective systems generated by the interaction of  
235 the cold pool outflow and the land breeze, based on high-resolution surface wind data  
236 retrieved by the CCMP and the ERA-interim temperature field.

237

#### 238 4.     **Summary**

239 This study analyzed the oceanic convective system that caused heavy rainfall  
240 over the western coast of Sumatra on 28 October 2007. The convective system satisfied  
241 the criteria for an MCC, as defined by Maddox (1980), and followed the developmental  
242 stages outlined by Cotton et al. (1989). The MCC developed from around midnight on  
243 27 October until the early morning of 28 October. Several convective systems were  
244 generated during the decay stage of the MCC because of convergence between the land  
245 breeze and westerly wind. The new convective systems around the decaying MCC were  
246 generated during the daytime on 28 October, and they propagated toward the western  
247 coast of Sumatra during the evening of 28 October because of the divergent outflow  
248 from the cold pool. The combination of the land breeze from Sumatra and the cold pool  
249 outflow from the decaying MCC was a significant factor in the formation of the  
250 convective system that caused the heavy rainfall up to  $46 \text{ mm h}^{-1}$  over the western coast  
251 of Sumatra.

252

### 253 **Acknowledgments**

254 Professor Y. Kodama, who is currently experiencing a serious health problem,  
255 contributed substantially to this paper to such an extent that he should be considered a  
256 co-author. The authors are grateful to the National Institute of Aeronautics and Space  
257 (LAPAN), which is the institution where the first author works. The Ministry of  
258 Research and Technology of the Government of Indonesia provided a scholarship to the  
259 first author. Special thanks are offered to Prof. Yoshihiro Tachibana (Mie University,  
260 Japan), Prof. Hiroyuki Yamada (University of the Ryukyus, Japan), Dr. Masaki  
261 Katsumata (Japan Agency for Marine–Earth Science and Technology, Japan), and Dr.

262 Kim Dionne Whitehall (Howard University, USA), who have all offered critical  
263 comments and suggestions for the improvement of this paper.

264

## 265 **References**

266 Ando, K., T. Matsumoto, T. Nagahama, I. Ueki, Y. Takatsuki, and Y. Kuroda, 2005:  
267 Drift characteristics of a moored conductivity-temperature-depth sensor and  
268 correction of salinity data. *J. Atmos. Oceanic Technol.*, **22**, 282-291.

269

270 Adler, R. F., and A. J. Negri, 1988: A satellite infrared technique to estimate tropical  
271 convective and stratiform rainfall. *J. Appl. Meteor.*, **27**, 30-51, doi:  
272 10.1175/1520-0450(1988)027<0030:ASITTE>2.0.CO;2.

273

274 Atlas, R., R. N. Hoffman, J. Ardizzone, S. M. Leidner, J. C. Jusem, D. K. Smith, and D.  
275 Gombos, 2011: A cross-calibrated, multiplatform ocean surface wind velocity  
276 product for meteorological and oceanographic applications. *Bull. Amer. Meteor.*  
277 *Soc.*, **92**, 157-174. doi: 10.1175/2010BAMS2946.1.

278

279 Cotton, W. R., M. S. Lin, R. L. McAnelly, and C. J. Tremback, 1989: A composite  
280 model of mesoscale convective complexes. *Mon. Wea. Rev.*, **116**, 939-949, doi:  
281 10.1175/1520-0493(1989)117<0765:ACMOMC>2.0.CO;2.

282

283 Dee, D. P., S. M. Uppala, A. J. Simmons, P. Berrisford, P. Poli, S. Kobayashi, U.  
284 Andrae, M. A. Balmaseda, G. Balsamo, P. Bauer, P. Bechtold, A. C. M. Beljaars,  
285 L. van de Berg, J. Bidlot, N. Bormann, C. Delsol, R. Dragani, M. Fuentes, A. J.

286 Geer, L. Haimberger, S. B. Healy, H. Hersbach, E. V. Holm, L. Isaksen, P.  
287 Kallberg, M. Kohler, M. Matricardi, A. P. McNally, B. M. Monge-Sanz, J. J.  
288 Morcrette, B. K. Park, C. Peubey, P. de Rosnay, C. Tavalato, J. N. Thepaut, and  
289 F. Vitart, 2011: The ERA-Interim reanalysis: configuration and performance of  
290 the data assimilation system. *Quart. J. Roy. Meteor. Soc.*, **137**, 553-597, doi:  
291 10.1002/qj.828.

292

293 Engerer, N. A., D. J. Stensrud, and M. C. Coniglio, 2008: Surface characteristics of  
294 observed cold pools. *Mon. Wea. Rev.*, **136**, 4839-4849, doi:  
295 10.1175/2008MWR2528.1.

296

297 Hirose, M., R. Oki, A. D. Short, and K. Nakamura, 2009: Regional characteristics of  
298 scale-based precipitation systems from ten years of TRMM PR data. *J. Meteor.*  
299 *Soc. Japan.*, **87A**, pp. 353-368, doi: 10.2151/jmsj.87A.353.

300

301 Houze, R. A., S. G. Geotis, F. D. Marques, and A. K. West, 1981: Winter monsoon  
302 convection in the vicinity of north Borneo. Part I: Structure and time variation of  
303 the clouds and precipitation. *Mon. Wea. Rev.*, **109**, 1595–1614, doi:  
304 10.1175/1520-0493(1981)109<1595:WMCITV>2.0.CO;2.

305

306 Houze, R. A., Jr., 2004: Mesoscale convective systems. *Rev. Geophys.*, **42**,  
307 10.1029/2004RG000150, 43 pp.

308

309 Love, B. S., A. J. Matthews, G. M. S. Lister, 2011: The diurnal cycle of precipitation  
310 over the Maritime Continent in a high-resolution atmospheric model. *Quart. J.*  
311 *Roy. Meteor. Soc.*, **137**, 934-947, doi: 10.1002/qj.809.

312

313 Maddox, R. A., 1980: Mesoscale convective complexes. *Bull. Amer. Meteor. Soc.*, **61**,  
314 1374-1387.

315

316 Mori, S., Hamada J.-I., Y. I. Tauhid, M. D. Yamanaka, N. Okamoto, F. Murata, N.  
317 Sakurai, H. Hashiguchi, and T. Sribimawati, 2004: Diurnal land-sea rainfall  
318 peak migration over Sumatra Island, Indonesian Maritime Continent, observed  
319 by TRMM satellite and intensive rawinsonde soundings. *Mon. Wea. Rev.*, **132**,  
320 2021-2039.

321

322 Mori, S., Hamada J.-I., N. Sakurai, H. Fudeyasu, M. Kawashima, H. Hashiguchi, F.  
323 Syamsudin, A. A. Arbain, R. Sulistyowati, J. Matsumoto, and M. D. Yamanaka,  
324 2011: Convective systems developed along the coastline of Sumatra Island,  
325 Indonesia, observed with an x-band doppler radar during the HARIMAU2006  
326 campaign. *J. Meteor. Soc. Japan.*, **89A**, 61-81, doi:10.2151/jmsj.2011-A04.

327

328 Nakazawa, T., 1988: Tropical super clusters within intraseasonal variations over the  
329 western Pacific. *J. Meteor. Soc. Japan.*, **66**, 823-839.

330

331 Nitta, T., and S. Sekine, 1994: Diurnal variation of convective activity over tropical  
332 western Pacific. *J. Meteor. Soc. Japan.*, **72**, 627-641.

333

334 Ramage, C. S., 1968: Role of a "Maritime Continent" in the atmospheric circulation.

335 *Mon. Wea. Rev.*, **96**, 365-370, doi: 10.1175/1520-

336 0493(1968)096<0365:ROATMC>2.0.CO;2.

337

338 Sakurai, N., F. Murata, M. D. Yamanaka, S. Mori, J. I. Hamada, H. Hashiguchi, Y. I.

339 Tauhid, T. Sribimawati, and B. Suhardi, 2005: Diurnal cycle of cloud system

340 migration over Sumatra Island. *J. Meteor. Soc. Japan.*, **83**, 835-850.

341

342 Shibagaki, Y., T. Shimomai, T. Kozu, S. Mori, Y. Fujiyoshi, H. Hashiguchi, M. K.

343 Yamamoto, S. Fukao, and M. D. Yamanaka, 2006: Multi-scale aspects of

344 convective systems associated with an intraseasonal oscillation over the

345 Indonesian Maritime Continent. *Mon. Wea. Rev.*, **134**, 1682-1696, doi:

346 10.1175/MWR3152.1.

347

348 Tompkins, A.M.,2001: Organization of tropical convection in low vertical wind shears:

349 the role of cold pools. *J. Atmos. Sci.*, **58**, 1650-1672.

350

351 Valor G.B., and D. J. M. G. López, 2014: OGIMET – professional information about

352 meteorological conditions in the world. <http://www.ogimet.com>, (accessed 24

353 March 2015).

354

355 Virts, K. S., and R. A. Houze, Jr., 2015: Variation of lightning and convective rain  
356 fraction in mesoscale convective systems of the MJO. *J. Atmos. Sci.*, **72**, 1932-  
357 1944, doi: 10.1175/JAS-D-14-0201.1.

358

359 Wheeler, M. C., and H. H. Hendon, 2004: An all-season real-time multivariate MJO  
360 index: Development of an index for monitoring and prediction. *Mon. Wea. Rev.*,  
361 **132**, 1917-1932.

362

363 Williams, M., and R. A. Houze Jr., 1987: Satellite-observed characteristics of winter  
364 monsoon cloud clusters. *Mon. Wea. Rev.*, **115**, 505-519, doi: 10.1175/1520-  
365 0493(1987)115<0505:SOCOWM>2.0.CO;2.

366

367 Wilson, J. W. and W. E. Schreiber, 1986: Initiation of convective storms at radar-  
368 observed boundary-layer convergence lines. *Mon. Wea. Rev.*, **114**, 2516-2536,  
369 doi: 10.1175/1520-0493(1986)114<2516:IOCSAR>2.0.CO;2

370

371 Yamanaka, M. D., H. Hashiguchi, S. Mori, P. Wu, F. Syamsudin, T. Manik, Hamada J.-  
372 I., M. K. Yamamoto, M. Kawashima, Y. Fujiyoshi, N. Sakurai, M. Ohi, R.  
373 Shirooka, M. Katsumata, Y. Shibagaki, T. Shimomai, Erlansyah, W. Setiawan,  
374 B. Tejasukmana, Y. S. Djajadihardja, and J. T. Anggadiredja, 2008: HARIMAU  
375 radar-profiler network over Indonesian maritime continent: A GEOSS early  
376 achievement for hydrological cycle and disaster prevention. *J. Disaster. Res.*, **3**,  
377 78-88.

378



379 Yuan, J., and R. A. Houze Jr., 2010: Global variability of mesoscale convective system  
380 anvil structure from A-Train satellite data. *J. Climate*, **23**, 5864-5888, doi:  
381 10.1175/2010JCLI3671.1

382

383

#### 384 **Figure Captions**

385 **Fig. 1.** Horizontal distribution of black body temperature ( $T_{BB}$ ) for Mesoscale  
386 Convective Complex (MCC) criteria from infrared data obtained by MTSAT-1R  
387 over the Indian Ocean near Sumatra on 27–28 October 2007, showing the eight  
388 stages of MCC evolution: (a) MCC-12h stage (1000 local time (LT)), 27 October  
389 2007; (b) pre-MCC stage (2200 LT), 27 October 2007; (c) initial stage (0100 LT),  
390 28 October 2007; (d) growth stage (0400 LT), 28 October 2007; (e) mature stage  
391 (0700 LT), 28 October 2007; (f) decay stage (1300 LT), 28 October 2007; (g)  
392 dissipation stage (1600 LT), 28 October 2007; (h) post-MCC stage (1900 LT), 28  
393 October 2007. Red color indicates interior cold cloud with  $T_{BB} \leq 221$  K and blue  
394 color indicates cloud shield with  $T_{BB} \leq 241$  K. Tb, ST, PB and PK are respectively  
395 Tabing, Simpang-tiga, Pulau Baai and Padang Kemiling shows the location of  
396 weather stations.

397

398 **Fig. 2.** Horizontal distribution of convective index ( $C_i$ ) (shaded) from infrared data of  
399 MTSAT-1R, wind surface vector anomaly (vector) from Cross-Calibrated Multi-  
400 Platform (CCMP) data, and potential temperature (contour) from the European  
401 Centre for Medium-Range Weather Forecasts (ECMWF) ERA-Interim data during  
402 the occurrence of the Mesoscale Convective Complex (MCC) over the Indian

403 Ocean near Sumatra on 28 October 2007: (a) initial stage (0100 local time (LT)),  
404 showing merging of some convective clouds to create the MCC; (b) mature stage  
405 (0700 LT), showing cold pool area forming in the center of the MCC, as indicated  
406 by the low potential temperature; (c) decay stage (1300 LT), showing several new  
407 convective systems forming on the leading edge of the cold pool; (d) post-MCC  
408 stage (1900 LT), showing the new convective systems migrating from over the  
409 Indian Ocean near Sumatra toward the western coast of Sumatra. Tb, ST, PB and  
410 PK are respectively Tabing, Simpang-tiga, Pulau Baai and Padang Kemiling  
411 shows the location of weather stations.

412

413 **Fig. 3.** Horizontal distribution of rainfall from Tropical Rainfall Measuring Mission  
414 (TRMM) 3B42 v6 data (shaded) and wind vector anomaly (vector) from Cross-  
415 Calibrated Multi-Platform (CCMP) data during the occurrence of the Mesoscale  
416 Convective Complex (MCC) over the Indian Ocean near Sumatra on 28 October  
417 2007: (a) initial stage (0100 local time (LT)); (b) mature stage (0700 LT); (c)  
418 decay stage (1300 LT); (d) dissipation stage (1600 LT) but when wind data were  
419 not available; and (e) post-MCC stage (1900 LT). Tb, ST, PB and PK are  
420 respectively Tabing, Simpang-tiga, Pulau Baai and Padang Kemiling shows the  
421 location of weather stations.

422

423 **Fig. 4.** Rainfall observational data during the occurrence of the Mesoscale Convective  
424 Complex (MCC) over the Indian Ocean near Sumatra on 28 October 2007 (1300–  
425 2400 local time (LT)) at specific sites on the western coast of Sumatra: Pulau Baai  
426 weather station in Bengkulu, Tabing weather station in Padang, Simpang-tiga

427 weather station in Pekanbaru, and Padang Kemiling weather station in Bengkulu.

428 The figure panel shows the location of weather stations.

429

430 **Fig. 5.** Schematic representations of the evolution and migration of the mesoscale

431 convective complex (MCC) over the Indian Ocean near Sumatra related to the

432 diurnal rainfall variation over the western coast of Sumatra. (a) MCC initial stage

433 around midnight; (b) MCC mature stage during the morning; (c) MCC decay stage

434 during the daytime; and (d) MCC dissipation stage during the evening. Light and

435 dark gray areas indicate the MCC cloud shield and convective clouds, respectively.

436 Cores of heavy rainfall are represented by green circles. Convergent and divergent

437 flows are indicated by the blue and red arrows, respectively. The cold pools in (b)

438 and (c) are indicated by blue ellipses.

439

440

441

**Table 1. Physical characteristics of MCCs (Maddox 1980)**

<i>Size:</i>	A-Cloud shield with continuously low $T_{BB} \leq -32^{\circ}\text{C}$ (241 K) must have an area $\geq 100,000 \text{ km}^2$ B-Interior cold cloud region with $T_{BB} \leq -52^{\circ}\text{C}$ (221 K) must have an area $\geq 50,000 \text{ km}^2$
<i>Initiate:</i>	Size definitions A and B are first satisfied
<i>Duration:</i>	Size definition A and B must be met for a period of $\geq 6$ hours
<i>Maximum extent:</i>	Contiguous cold cloud shield ( $T_{BB} \leq -32^{\circ}\text{C}$ (241 K) ) reaches a maximum size
<i>Shape:</i>	Eccentricity (minor axis/major axis) $\geq 0.7$ at time of maximum extent
<i>Terminate:</i>	Size definitions A and B no longer satisfied

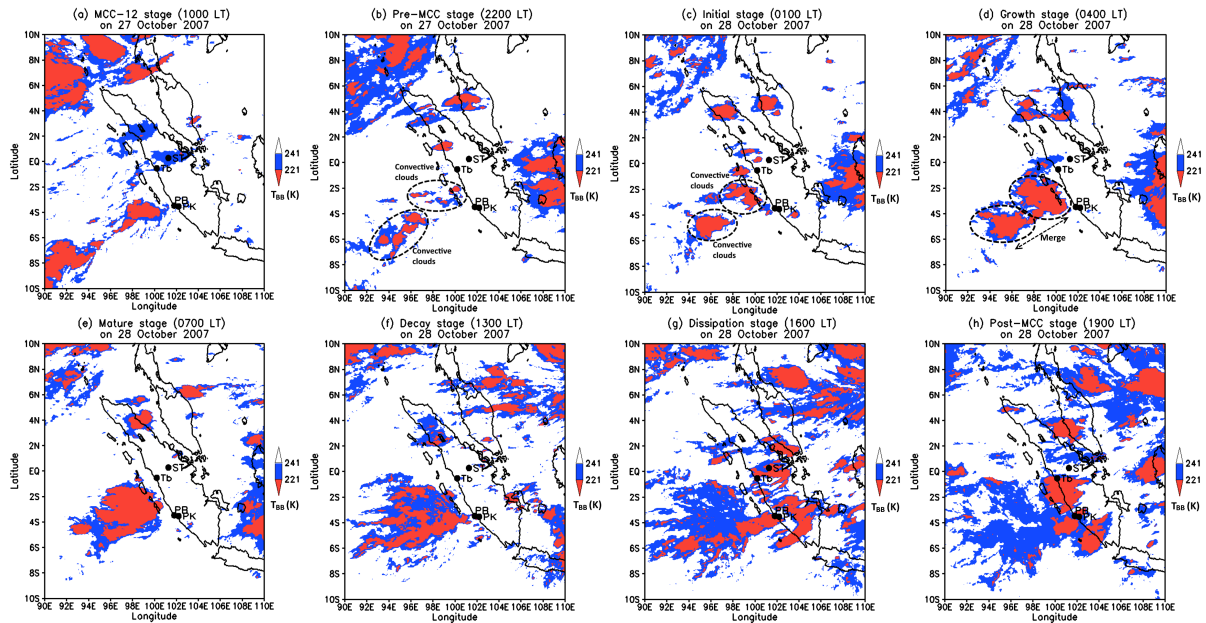


**Fig. 1.** Horizontal distribution of black body temperature ( $T_{BB}$ ) for Mesoscale Convective Complex (MCC) criteria from infrared data obtained by MTSAT-1R over the Indian Ocean near Sumatra on 27–28 October 2007, showing the eight stages of MCC evolution: (a) MCC-12h stage (1000 local time (LT)), 27 October 2007; (b) pre-MCC stage (2200 LT), 27 October 2007; (c) initial stage (0100 LT), 28 October 2007; (d) growth stage (0400 LT), 28 October 2007; (e) mature stage (0700 LT), 28 October 2007; (f) decay stage (1300 LT), 28 October 2007; (g) dissipation stage (1600 LT), 28 October 2007; (h) post-MCC stage (1900 LT), 28 October 2007. Red color indicates interior cold cloud with  $T_{BB} \leq 221$  K and blue color indicates cloud shield with  $T_{BB} \leq 241$  K. Tb, ST, PB and PK are respectively Tabing, Simpang-tiga, Pulau Baai and Padang Kemiling shows the location of weather stations.

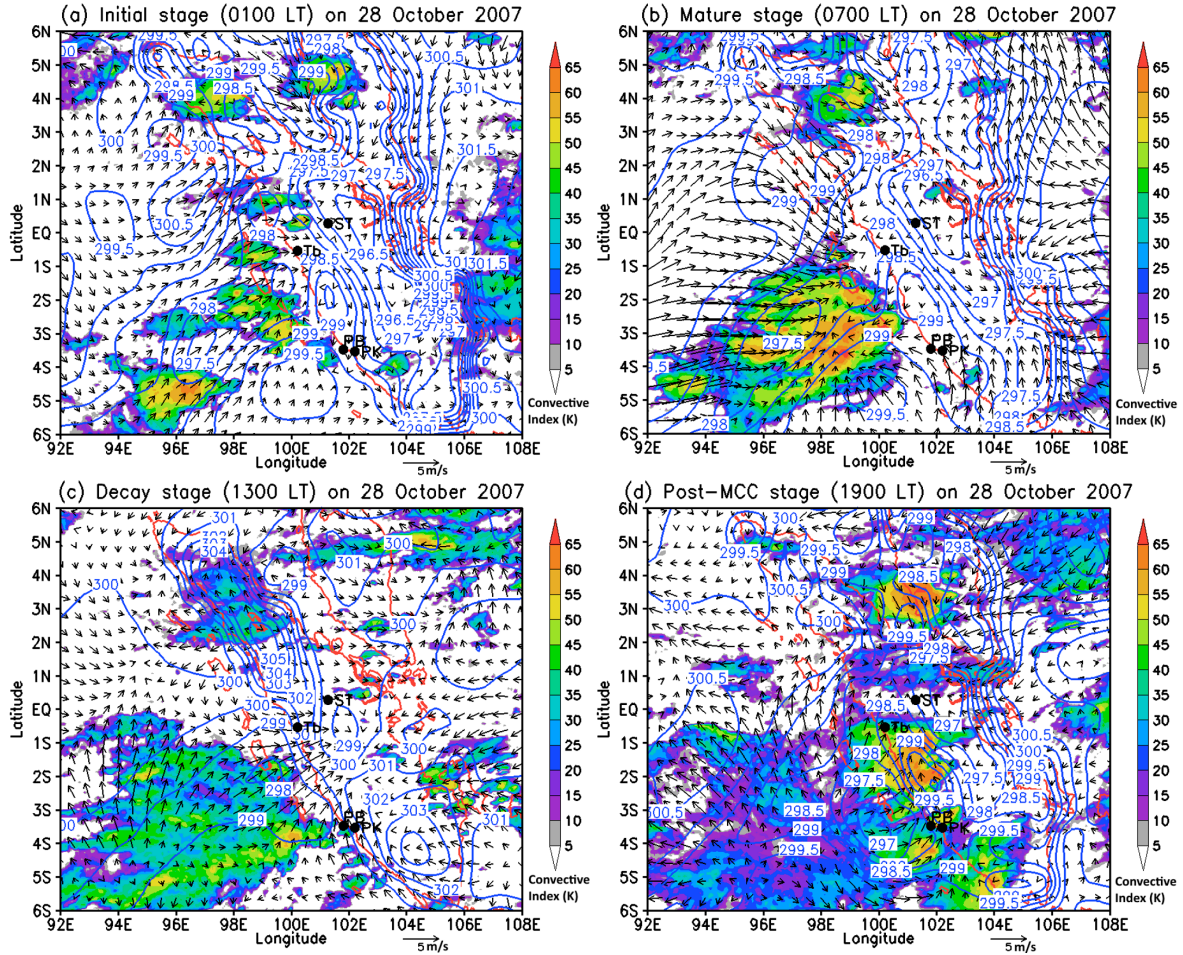


**Fig. 2.** Horizontal distribution of convective index ( $C_i$ ) (shaded) from infrared data of MTSAT-1R, wind surface vector anomaly (vector) from Cross-Calibrated Multi-Platform (CCMP) data, and potential temperature (contour) from the European Centre for Medium-Range Weather Forecasts (ECMWF) ERA-Interim data during the occurrence of the Mesoscale Convective Complex (MCC) over the Indian Ocean near Sumatra on 28 October 2007: (a) initial stage (0100 local time (LT)), showing merging of some convective clouds to create the MCC; (b) mature stage (0700 LT), showing cold pool area forming in the center of the MCC, as indicated by the low potential temperature; (c) decay stage (1300 LT), showing several new convective systems forming on the leading

edge of the cold pool; (d) post-MCC stage (1900 LT), showing the new convective systems migrating from over the Indian Ocean near Sumatra toward the western coast of Sumatra. Tb, ST, PB and PK are respectively Tabing, Simpang-tiga, Pulau Baai and Padang Kemiling shows the location of weather stations.

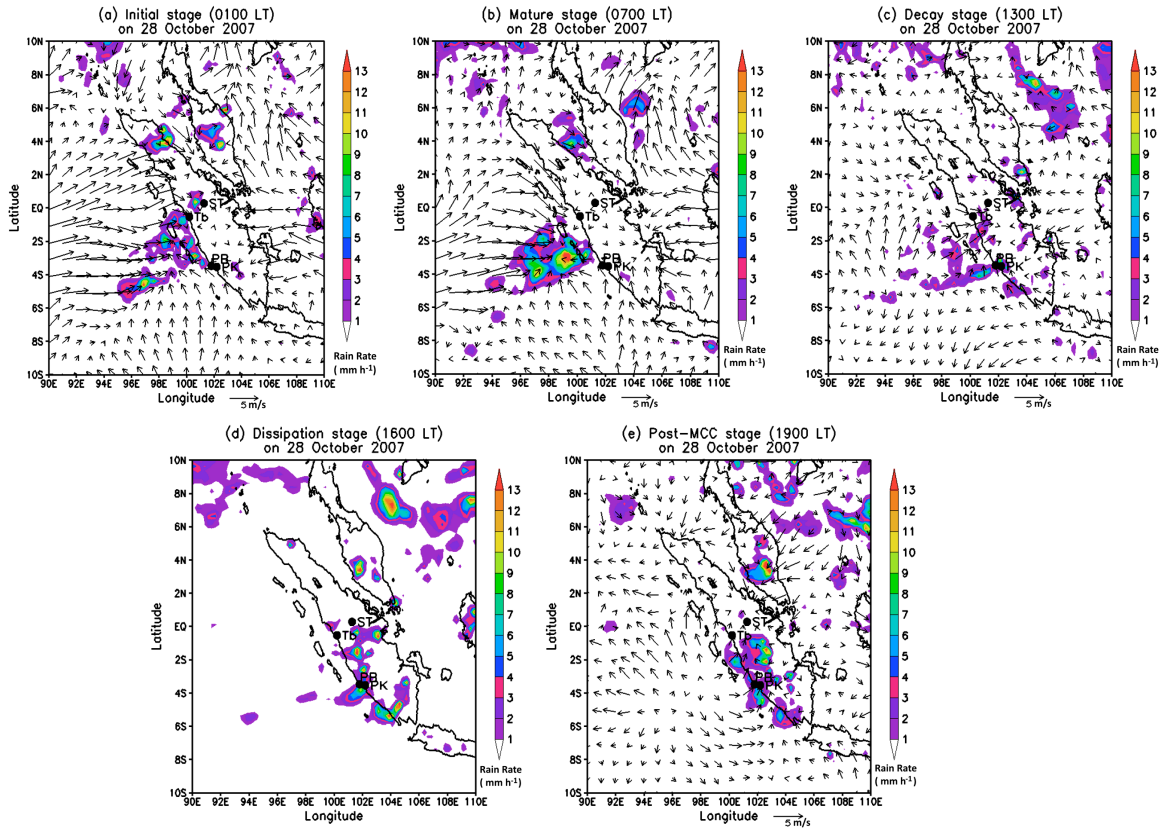


**Fig. 3.** Horizontal distribution of rainfall from Tropical Rainfall Measuring Mission (TRMM) 3B42 v6 data (shaded) and wind vector anomaly (vector) from Cross-Calibrated Multi-Platform (CCMP) data during the occurrence of the Mesoscale Convective Complex (MCC) over the Indian Ocean near Sumatra on 28 October 2007: (a) initial stage (0100 local time (LT)); (b) mature stage (0700 LT); (c) decay stage (1300 LT); (d) dissipation stage (1600 LT) but when wind data were not available; and (e) post-MCC stage (1900 LT). Tb, ST, PB and PK are respectively Tabing, Simpang-

tiga, Pulau Baai and Padang Kemiling shows the location of weather stations.

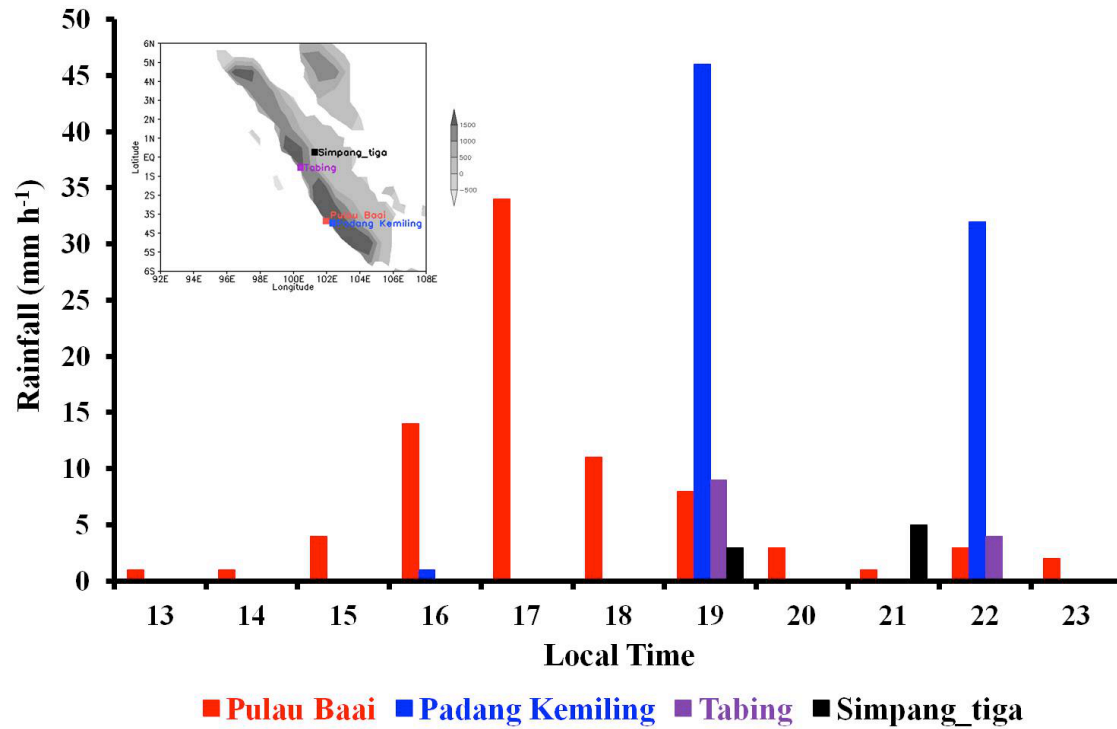


**Fig. 4.** Rainfall observational data during the occurrence of the Mesoscale Convective Complex (MCC) over the Indian Ocean near Sumatra on 28 October 2007 (1300–2400 local time (LT)) at specific sites on the western coast of Sumatra: Pulau Baai weather station in Bengkulu, Tabing weather station in Padang, Simpang Tiga weather station in Pekanbaru, and Padang Kemiling weather station in Bengkulu. The figure panel shows the location of weather stations.



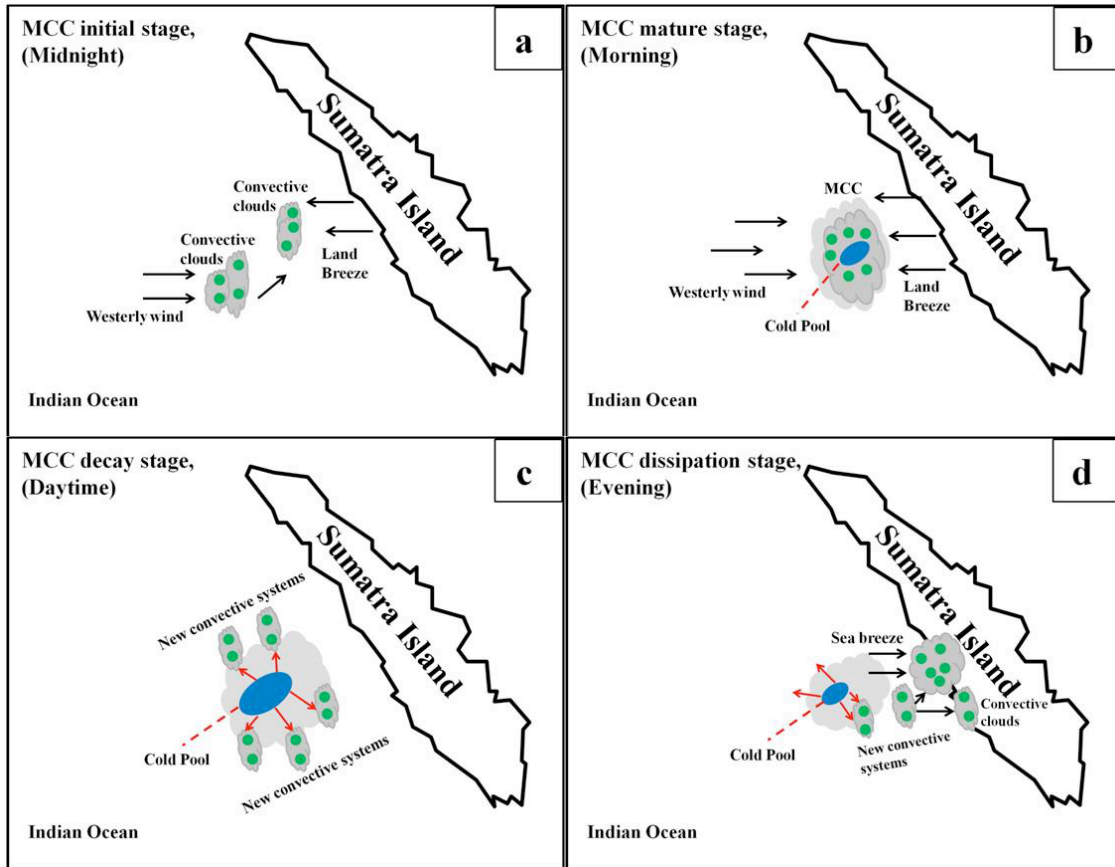


**Fig. 5.** Schematic representations of the evolution and migration of the mesoscale convective complex (MCC) over the Indian Ocean near Sumatra related to the diurnal rainfall variation over the western coast of Sumatra. (a) MCC initial stage around midnight; (b) MCC mature stage during the morning; (c) MCC decay stage during the daytime; and (d) MCC dissipation stage during the evening. Light and dark gray areas indicate the MCC cloud shield and convective clouds, respectively. Cores of heavy rainfall are represented by green circles. Convergent and divergent flows are indicated by the blue and red arrows, respectively. The cold pools in (b) and (c) are indicated by blue ellipses.